Inorganic Chemistry

ARTICLE

pubs.acs.org/IC

Specific Incorporation of Chalcogenide Bridge Atoms in Molybdenum/Tungsten-Iron-Sulfur Single Cubane Clusters

Amit Majumdar and R. H. Holm*

Department of Chemistry and Chemical Biology, Harvard University, Cambridge, Massachusetts 02138, United States

Supporting Information

ABSTRACT: An extensive series of heterometal-iron-sulfur single cubane-type clusters with core oxidation levels $[MFe_3S_3Q]^{3+,2+}$ (M = Mo, W; Q = S, Se) has been prepared by means of a new method of cluster self-assembly. The procedure utilizes the assembly system $[(^tBu_3tach)M^{VI}S_3]/FeCl_2/Na_2Q/NaSR$ in acetonitrile/THF and affords product clusters in 30−50% yield. The trisulfido precursor acts as a template, binding Fe^{II} under reducing conditions and supplying the MS_3 unit of the product. The system leads to specific incorporation of a μ_3-chalcogenide from an external source (Na_2Q) and affords the products $[(^tBu_3tach)MFe_3S_3QL_3]^{0/1-}$ ($L = Cl^-, RS^-$), among which are the first MFe_3S_3Se clusters prepared. Some 16 clusters have been prepared, 13 of which have been characterized by X-ray structure determinations including the incomplete cubane $[(^tBu_3tach)MoFe_2S_3Cl_2(\mu_2\text{-}SPh)]$, a possible trapped intermediate in the assembly process. Comparisons of structural and electronic features of clusters differing only in atom Q at one cubane vertex are provided. In comparative pairs of complexes differing only in Q, placement of one selenide atom in the core increases core volumes by about 2% over the Q = S case, sets the order Q = Se > S in Fe-Q bond lengths and Q = S > Se in Fe-Q-Fe bond angles, causes small positive shifts in redox potentials, and has an essentially nil effect on ^{57}Fe isomer shifts. Iron mean oxidation states and charge distributions are assigned to most clusters from isomer shifts. ($^tBu_3tach$ = 1,3,5-*tert*-butyl-1,3,5-triazacyclohexane)

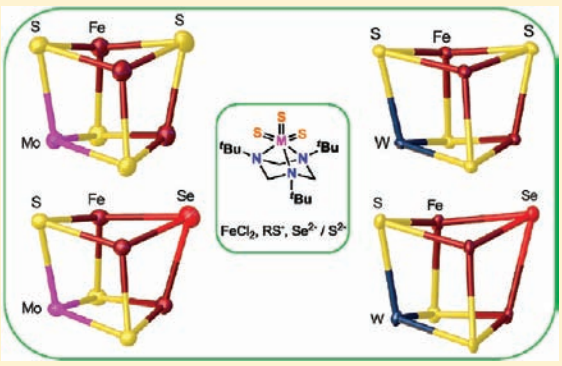

INTRODUCTION

The large majority of homo- and heterometallic iron-sulfur clusters of biomimetic relevance are synthesized under three protocols:[1] (i) self-assembly, consisting of self-organizing reactions between simple mononuclear precursors and ligand reagents, and (ii) fragment condensation in which a preformed di- or polynuclear cluster reacts with a mononuclear species, itself, or another cluster. Certain clusters formed by these methods can undergo (iii) core rearrangement, reorganization of a pre-existing cluster from (i) or (ii) to a different core geometry. Examples include formation of $Fe_3S(SR)_3$,[2] Fe_4S_4,[3−5] and MFe_3S_4 (M = Mo, W)[1,6,7] clusters by self-assembly, MFe_3S_4 (M = V,[8] Ni[9,10]), and $M_2Fe_6S_8$ (M = Fe,[11,12] Mo,[13−15]) clusters by fragment condensation, and $M_2Fe_6S_9$ clusters (M = Mo,[16,17] V[18]) by core rearrangement. Frequently, clusters employed in fragment condensation are prepared by self-assembly, in which the bridging ligand reagent is metal-bound or free sulfide, hydrosulfide, sulfur, RSSR, or RSSSR and a reductant, or $(R_3Si)_2S$. Cluster products obtained in this way have the invariant feature of bridging sulfide core atoms, always of the μ_3-S mode when the core structure adopts the prevalent cubane-type geometry. Recent advances in synthesis have afforded new types of clusters with internal ($M_2Fe_6S_9$) and interstitial (Fe_8S_7)[19−21] μ_6-S bridge components.

The foregoing high-nuclearity clusters are directly pertinent to synthetic endeavors directed toward the P^N (Fe_8S_7) and FeMo-cofactor ($MoFe_7S_9X$) clusters of nitrogenase which contain internal μ_6-S and interstitial μ_6-X (X = C, N, or O) bridging elements, respectively.[22−24] A largely unsolved problem is the deliberate installation of nonsulfur bridge atoms (preferably X) in clusters of nuclearity four and higher. If the problem is approached with less complex cubane-type species, $Fe_4(\mu_3\text{-}Se)_4$[25−34] and MFe_3Se_4 (M = Mo, W)[35] clusters, prepared by self-assembly, become relevant as a first step in that direction. Lee and co-workers have made significant progress by preparation of two unprecedented types of cubane-type clusters, $Fe_4(NR)_4$ by self-assembly,[36,37] and the mixed-ligand clusters $Fe_4S_n(NR)_{4-n}$ (n = 1−3) by remarkable fragment condensation reactions.[38] The latter results are noteworthy because of the first successful introduction of nitrogen bridges (as imides) and the isolation of clusters with mixed-atom bridges. Early in the development of iron-sulfur cluster chemistry, it was shown that the clusters $[Fe_4Q_4(SR)_4]^{2-/3-}$ (Q = S, Se) sustain core atom exchange reactions to form $[Fe_4S_nSe_{4-n}(SR)_4]^{2-/3-}$ in solution; mixed bridge atom clusters were detected by ^{1}H NMR but not isolated.[26]

Recently, we have been experimenting with a new type of cluster assembly reaction based on trisulfido complexes of general formulation $[L_3M^{VI}S_3]^{0,1-}$. These are intended to act as templates

Received: August 18, 2011
Published: October 10, 2011

Chart 1. Abbreviations and Designation of Compounds

[(^{t}Bu$_3$tach)MS$_3$]	**1a** (M = Mo),[39] **1b** (M = W)[39]
[(^{t}Bu$_3$tach)MoFe$_2$S$_3$Cl$_2$(μ_2-SPh)]	**2**
[(^{t}Bu$_3$tach)MoFe$_3$S$_4$Cl$_3$]	**3**
[(^{t}Bu$_3$tach)MFe$_3$S$_3$QCl$_2$(SPh)]	**4a** (M = Mo, Q = S), **4b** (M = Mo, Q = Se)
	5a (M = W, Q = S), **5b** (M = W, Q = Se)
[(^{t}Bu$_3$tach)MFe$_3$S$_3$Q(SEt)$_3$]	**6** (M = Mo, Q = S)
	7a (M = W, Q = S), **7b** (M = W, Q = Se)
[(^{t}Bu$_3$tach)MoFe$_3$S$_3$Q(SMe)$_3$]Na[a]	**8a** (Q = S), **8b** (Q = Se)
[(^{t}Bu$_3$tach)MoFe$_3$S$_3$Q(SEt)$_3$]Na[b]	**9a** (Q = S), **9b** (Q = Se)
[(^{t}Bu$_3$tach)MFe$_3$S$_3$Q(SPh)$_3$]	**10a** (M = Mo, Q = S), **10b** (M = Mo, Q = Se)
	11a (M = W, Q = S), **11b** (M = W, Q = Se)

^{t}Bu$_3$tach =1,3,5-tri-*tert*-butyl-1,3,5-triazacyclohexane; Me$_3$tacn =1,4,7-trimethyl-1,4,7-triazacyclononane; Tp* = tris(3,5-dimethylpyrazolyl)-hydroborate(1-). [a] Minimal formula; the X-ray structure shows a dimeric form involving two Na$^+$ each coordinated by one Et$_2$O molecule of half-occupancy. [b] Minimal formula; X-ray structure shows three acetonitrile molecules coordinated to Na$^+$.

in cluster self-assembly by providing in the product cluster a desired metal-trisulfido fragment MS$_3$ which supports metal binding when reduced and whose other coordination sites are protected by a tridentate ligand L$_3$. This work utilizes the compounds [(^{t}Bu$_3$tach)M^{VI}S$_3$] (M = Mo, W; see Chart 1 for abbreviations) prepared in this laboratory.[39] Assembly reaction systems allow specific incorporation of a single selenide atom leading to cores of the type MS$_3$Se that may be isolated in stable clusters. We report the synthesis, structures, and selected properties of such clusters.

■ EXPERIMENTAL SECTION

Preparation of Compounds. All reactions and manipulations were performed under a pure dinitrogen atmosphere using either Schlenk techniques or an inert atmosphere box. Solvents were passed through an Innovative Technology solvent purification system prior to use. In the preparations that follow, reactants were nearly always used as suspensions in solvents of specified volume, filtrations were through Celite, solvent removal steps were performed in vacuo, and products were washed with ether and dried. Sodium sulfide, sodium selenide, and ferrous chloride were used in anhydrous form from commercial sources. All new compounds were identified by combinations of ^{1}H NMR spectroscopy (in Me$_2$SO-d$_6$), X-ray structure determinations, and elemental analysis (Midwest Microlab, LLC, Indianapolis, IN 46250). Neutral compounds with three thiolate ligands are soluble in acetonitrile, tetrahydrofuran (THF), and Me$_2$SO. Neutral compounds with one thiolate or no thiolate ligand and cluster salts are soluble in acetonitrile and Me$_2$SO. All compounds are extremely air-sensitive and must be handled accordingly.

[(^{t}Bu$_3$tach)MoFe$_2$S$_3$Cl$_2$(μ_2-SPh)]. To a suspension of [(^{t}Bu$_3$tach)MoS$_3$][39] (45 mg, 0.10 mmol) in 1 mL of methanol was added a solution of NaSPh (27 mg, 0.20 mmol) in 2 mL of methanol followed by a solution of FeCl$_2$ (25 mg, 0.20 mmol) in 5 mL of methanol. The reaction mixture was stirred for 12 h. The red-brown solution was evaporated to dryness, the solid was extracted with 5 mL of THF, and the extract was filtered. The volume of the filtrate was reduced to about 0.5 mL, affording the product as a black crystalline solid (35 mg, 47%) which sometimes contained an impurity of [(^{t}Bu$_3$tach)MoFe$_3$S$_4$Cl$_3$]. The compound was identified by an X-ray structure determination.

[(^{t}Bu$_3$tach)MoFe$_3$S$_4$Cl$_3$]. To [(^{t}Bu$_3$tach)MoS$_3$] (45 mg, 0.10 mmol) in 1 mL of acetonitrile was added NaSPh (13 mg, 0.10 mmol) in 2 mL of acetonitrile followed by Na$_2$S (12 mg, 0.15 mmol) in 2 mL of acetonitrile. FeCl$_2$ (38 mg, 0.30 mmol) in 5 mL of THF was immediately added to the solution, and the reaction mixture was stirred for 36 h. The red-brown solution was evaporated to dryness, the solid was extracted with 5 mL of acetonitrile, and the extract was filtered. The filtrate was evaporated to dryness. The residue was dissolved in 1 mL of acetonitrile, the solution was filtered, and the filtrate was diffused with ether at −35 °C for 2 d. The product was obtained as a black crystalline solid (32 mg, 40%), occasionally with the preceding cluster as an impurity. The compound was identified by an X-ray structure determination.

[(^{t}Bu$_3$tach)MoFe$_3$S$_4$Cl$_2$(SPh)]. To [(^{t}Bu$_3$tach)MoS$_3$] (45 mg, 0.10 mmol) in 1 mL of acetonitrile was added NaSPh (27 mg, 0.20 mmol) in 2 mL of acetonitrile followed by Na$_2$S (12 mg, 0.15 mmol) in 2 mL of acetonitrile. FeCl$_2$ (38 mg, 0.3 mmol) in 5 mL of THF was immediately added, and the reaction mixture was stirred for 36 h. The red-brown solution was evaporated to dryness, the residue was extracted with 5 mL of acetonitrile, and the extract was filtered. The filtrate was evaporated to dryness. The residue was dissolved in 1 mL of acetonitrile, filtered, and diffused with ether at −35 °C for 2 d to give the product as a black crystalline solid (25 mg, 30%). ^{1}H NMR: δ 14.60 (*m*-H, 2), 3.33 (CH$_2$, 6), 2.48 (CH$_3$, 27), −2.00 (*o*-H, 2), −4.18 (*p*-H, 1).

[(^{t}Bu$_3$tach)WFe$_3$S$_4$Cl$_2$(SPh)]. The preceding method on the same scale but with use of [(^{t}Bu$_3$tach)WS$_3$][39] was followed. The product was isolated as a black crystalline solid (28 mg, 30%). ^{1}H NMR: δ 14.23 (*m*-H, 2), 3.34 (CH$_2$, 6), 2.73 (CH$_3$, 27), −3.60 (*o*-H, 2), −3.99 (*p*-H, 1)

[(^{t}Bu$_3$tach)MoFe$_3$S$_3$SeCl$_2$(SPh)]. The procedure on the same scale for [(^{t}Bu$_3$tach)MoFe$_3$S$_4$Cl$_2$(SPh)] was followed but with use of Na$_2$Se (19 mg, 0.15 mmol) and no Na$_2$S added. The product was obtained as a black crytalline solid (30 mg, 35%). ^{1}H NMR: δ 14.60 (*m*-H, 2), 3.33 (CH$_2$, 6), 2.48 (CH$_3$, 27), −1.71 (*o*-H, 2), −4.27 (*p*-H, 1).

[(^{t}Bu$_3$tach)WFe$_3$S$_3$SeCl$_2$(SPh)]. The preceding method on the same scale for [(^{t}Bu$_3$tach)WFe$_3$S$_4$Cl$_2$(SPh)] was employed but with use of Na$_2$Se (19 mg, 0.15 mmol) and no Na$_2$S added. The product was obtained as a black crystalline solid (30 mg, 31%). ^{1}H NMR: δ 14.25 (*m*-H, 2), 3.34 (CH$_2$, 6), 2.48 (CH$_3$, 27), −3.47 (*o*-H, 2), −4.11 (*p*-H, 1).

[(^{t}Bu$_3$tach)MoFe$_3$S$_4$(SEt)$_3$]. To [(^{t}Bu$_3$tach)MoS$_3$] (45 mg, 0.10 mmol) in 1 mL of acetonitrile was added NaSEt (34 mg, 0.40 mmol) in 2 mL of acetonitrile followed by Na$_2$S (12 mg, 0.15 mmol) in 2 mL of acetonitrile. FeCl$_2$ (38 mg, 0.30 mmol) in 5 mL of THF was immediately added, and the reaction mixture was stirred for 36 h. The red-brown solution was evaporated to dryness, the solid was extracted with 5 mL of acetonitrile, and the extract was filtered. The filtrate was evaporated to dryness. The residue was dissolved in 1 mL of acetonitrile, filtered, and diffused with ether at −35 °C for 2 d, affording the product as a black crystalline solid (45 mg, 54%). ^{1}H NMR: δ 9.09 (SCH$_2$CH$_3$, 9), 3.30 (CH$_2$, 6), 2.06 (CH$_3$, 27), −8.44 (SCH$_2$CH$_3$, 6).

[(^{t}Bu$_3$tach)MoFe$_3$S$_4$(SEt)$_3$](Na). The preceding procedure on the same scale was used but with an increased amount of NaSEt (42 mg, 0.50 mmol). The compound was isolated as a black crystalline solid (55 mg, 52%). Anal. Calcd. for C$_{21}$H$_{48}$Fe$_3$MoN$_3$NaS$_7$: C, 29.55; H, 5.67; N, 4.92. Found: C, 30.03; H, 5.93; N, 4.51. ^{1}H NMR: δ 9.60 (SCH$_2$CH$_3$, 9), 3.30 (CH$_2$, 6), 2.05 (CH$_3$, 27), −9.32 (SCH$_2$CH$_3$, 6).

[(^{t}Bu$_3$tach)MoFe$_3$S$_4$(SMe)$_3$][Na(MeCN)]. The preceding method on the same scale was used but with NaSMe (35 mg, 0.50 mmol). The compound was isolated as a black crystalline solid (45 mg, 53%). ^{1}H NMR: δ 3.32 (CH$_2$, 6), 2.05 (CH$_3$, 27), −9.67 (SCH$_3$, 9). Anal. Calcd. for C$_{18}$H$_{42}$Fe$_3$MoN$_3$NaS$_7$·C$_2$H$_3$N: C, 28.18; H, 5.32; N, 6.57. Found: C, 28.56; H, 5.38; N, 6.34.

[(^{t}Bu$_3$tach)MoFe$_3$S$_3$Se(SEt)$_3$][Na(CH$_3$CN)$_3$]. To [(^{t}Bu$_3$tach)MoS$_3$] (45 mg, 0.10 mmol) in 1 mL of acetonitrile was added NaSEt (42 mg, 0.5 mmol) in 2 mL of acetonitrile followed by Na$_2$Se (19 mg, 0.15 mmol) in 2 mL of acetonitrile. FeCl$_2$ (38 mg, 0.3 mmol) in 5 mL of THF was immediately added, and the reaction mixture was stirred for 36 h. Reaction workup is the same as for the preceding sodium salt, yielding the product as a black crystalline solid (50 mg, 45%). ^{1}H NMR: δ 10.25 (SCH$_2$CH$_3$, 9), 3.30 (CH$_2$, 6), 1.36 (CH$_3$, 27), −8.48 (SCH$_2$CH$_3$, 6).

Table 1. Crystallographic Data for Compounds at 100 K[a] and 15 K[d] (7b)

	2	3	4a	4b	6	7b	8a
formula	$C_{21}H_{38}Cl_2Fe_2MoN_3S_4\cdot 1.5(CH_4O)$	$C_{15}H_{33}Cl_3Fe_3MoN_3S_4$	$C_{21}H_{38}Cl_2Fe_3MoN_3S_5$	$C_{21}H_{38}Cl_2Fe_3MoN_3S_4Se$	$C_{21}H_{48}Fe_3MoN_3S_7$	$C_{21}H_{48}Fe_3N_3S_6SeW$	$C_{18}H_{42}Fe_3MoN_3NaS_7\cdot 0.5(C_4H_{10}O)$
formula weight	787.42	753.56	827.28	874.17	830.6	965.39	848.57
crystal system	monoclinic	orthorhombic	monoclinic	monoclinic	monoclinic	orthorhombic	monoclinic
space group	*Cc*	*Pnma*	$P2_1$	$P2_1/n$	*Pc*	$Pna2_1$	$P2_1/n$
Z	2	4	2	4	2	4	2
a, Å	10.314(4)	18.3532(18)	14.516(3)	9.8517(8)	9.8714(19)	19.982(3)	9.8665(14)
b, Å	17.255(7)	14.7661(14)	10.013(2)	19.9821(17)	10.0395(19)	16.568(2)	20.871(3)
c, Å	19.572(9)	9.5624(9)	14.518(3)	17.4884(15)	19.241(3)	9.7591(12)	17.322(2)
α, deg	90	90	90	90	90	90	90
β, deg	93.301(9)	90	112.545(3)	90.024(2)	120.723(7)	90	91.349(3)
γ, deg	90	90	90	90	90	90	90
V, Å^3	3477(3)	2591.5(4)	1948.9(7)	3442.7(5)	1639.2(5)	3230.8(7)	3566.0(9)
d_{calcd}, g/cm^3	1.504	1.931	1.410	1.687	1.683	1.985	1.581
μ, mm^{-1}	1.594	2.76	1.828	3.066	2.138	1.491	1.979
max, min peaks, e Å^{-3}	1.709, −1.416	3.720, −7.290	1.565, −1.106	1.173, −1.388	1.926, −1.138	4.204, −3.746	2.794, −2.199
2θ range, deg	4.16−51.46	4.44−51.48	3.38−51.5	3.1−51.44	4.06−51.4	1.86−32.46	3.06−51.42
R_1[b] (wR_2)[c]	0.0638(0.1040)	0.0687(0.1662)	0.0787(0.2229)	0.0801(0.1446)	0.0973(0.2010)	0.0659(0.1967)	0.0565(0.1549)
GOF (F^2)	1.082	1.062	1.065	1.086	1.035	1.039	1.067

[a] Mo Kα radiation (λ = 0.71073 Å). [b] $R_1 = \Sigma||F_o| - |F_c||/\Sigma|F_o|$. [c] $wR_2 = \{\Sigma[w(F_o^2 - F_c^2)^2]/\Sigma[w(F_o^2)^2]\}^{1/2}$. [d] Synchrotron source (λ = 0.41328 Å).

$[(^t\text{Bu}_3\text{tach})\text{MoFe}_3\text{S}_3\text{Se}(\text{SMe})_3][\text{Na}(\text{Et}_2\text{O})]$. The preceding method on the same scale was used but with NaSMe (35 mg, 0.50 mmol). The compound was isolated as a black crystalline solid (45 mg, 50%). ^{1}H NMR: δ 3.35 (CH_2, 6), 1.35 (CH_3, 27) −8.74 (SCH_3, 9). Anal. Calcd. for $C_{18}H_{42}Fe_3MoN_3NaS_6Se\cdot C_4H_{10}O$: C, 26.83; H, 5.29; N, 4.69. Found: C, 26.98; H, 5.09; H, 4.79.

$[(^t\text{Bu}_3\text{tach})\text{WFe}_3\text{S}_3\text{Se}(\text{SEt})_3]$. To $[(^t\text{Bu}_3\text{tach})\text{WS}_3]$ (54 mg, 0.10 mmol) in 1 mL of acetonitrile was added NaSEt (42 mg, 0.50 mmol) in 2 mL of acetonitrile followed by Na_2Se (19 mg, 0.15 mmol) in 2 mL of acetonitrile. $FeCl_2$ (38 mg, 0.30 mmol) in 5 mL of THF was immediately added, and the reaction mixture was stirred for 36 h. The workup procedure was the same as for $[(^t\text{Bu}_3\text{tach})\text{MoFe}_3\text{S}_4(\text{SEt})_3]$, yielding the product as a black crystalline solid (40 mg, 41%). Anal. Calcd. for $C_{21}H_{48}Fe_3N_3S_6SeW$: C, 26.13; H, 5.01; N, 4.35. Found: C, 26.02; H, 5.09; N, 4.33. ^{1}H NMR): δ 8.39 (SCH_2CH_3, 9), 3.29 (CH_2, 6), 1.52 (CH_3, 27), −7.72 (SCH_2CH_3, 6).

$[(^t\text{Bu}_3\text{tach})\text{WFe}_3\text{S}_4(\text{SEt})_3]$. The preceding method was followed on the same scale but with use of Na_2S (12 mg, 0.15 mmol) instead of Na_2Se, affording the product as black crystals (40 mg, 43%). ^{1}H NMR: δ 8.77 (SCH_2CH_3, 9), 3.35 (CH_2, 6H), 1.91 (CH_3, 27), −9.29 (SCH_2CH_3, 6).

$[(^t\text{Bu}_3\text{tach})\text{MoFe}_3\text{S}_4(\text{SPh})_3]$. To $[(^t\text{Bu}_3\text{tach})\text{MoS}_3]$ (45 mg, 0.1 mmol) in 1 mL of acetonitrile was added NaSPh (52 mg, 0.4 mmol) in 2 mL of acetonitrile followed by Na_2S (12 mg, 0.15 mmol) in 2 mL of acetonitrile. $FeCl_2$ (38 mg, 0.3 mmol) in 5 mL of THF was immediately added to the solution, and the reaction mixture was stirred for 36 h. The red-brown solution was evaporated to dryness, the solid was extracted with 5 mL of THF, and the extract was filtered. The filtrate was taken to dryness. The residue was dissolved in 1 mL of acetonitrile; the solution was filtered and diffused with ether at −35 °C for 2 d, affording the product as a black crystalline solid (33 mg, 31%). Anal. Calcd. for $C_{33}H_{48}Fe_3MoN_3S_7$: C, 40.66; H, 4.96; N, 4.31. Found: C, 39.55; H, 4.97; N, 4.45. ^{1}H NMR: δ 14.81 (*m*-H, 6), 3.31 (CH_2, 6), 2.48 (CH_3, 27), −2.68 (*o*-H, 6), −4.24 (*p*-H, 3).

$[(^t\text{Bu}_3\text{tach})\text{WFe}_3\text{S}_4(\text{SPh})_3]$. The preceding method was followed on the same scale but with use of $[(^t\text{Bu}_3\text{tach})\text{WS}_3]$. The product was obtained as a black crystalline solid (35 mg, 30%). ^{1}H NMR: δ 14.24 (*m*-H, 6), 3.31 (CH_2, 6), 2.71 (CH_3, 27), −3.63 (*o*-H, 6), −3.99 (*p*-H, 3).

$[(^t\text{Bu}_3\text{tach})\text{MoFe}_3\text{S}_3\text{Se}(\text{SPh})_3]$. To $[(^t\text{Bu}_3\text{tach})\text{MoS}_3]$ (45 mg, 0.10 mmol) in 1 mL of acetonitrile was added NaSPh (52 mg, 0.40 mmol) in 2 mL of acetonitrile followed by Na_2Se (19 mg, 0.15 mmol) in 2 mL of acetonitrile. A suspension of ferrous chloride (38 mg, 0.3 mmol) in 5 mL of THF was immediately added to the solution, and the reaction mixture was stirred for 36 h. The reaction workup followed that for $[(^t\text{Bu}_3\text{tach})\text{MoFe}_3\text{S}_4(\text{SPh})_3]$, leading to the product as a black solid (35 mg, 33%) which analyzed as an acetonitrile hemisolvate (in conformity with the X-ray structure). Anal. Calcd. for $C_{33}H_{48}Fe_3MoN_3S_6Se\cdot 0.5C_2H_3N$: C, 39.19; H, 4.79; N, 4.70. Found: C, 38.90; H, 4.69; N, 4.43. ^{1}H NMR: δ 14.75 (*m*-H, 6), 3.30 (CH_2, 6), 2.22 (CH_3, 27), −1.99 (*o*-H, 6), −4.28 (*p*-H, 3).

$[(^t\text{Bu}_3\text{tach})\text{WFe}_3\text{S}_3\text{Se}(\text{SPh})_3]$. The preceding procedure was employed but with use of $[(^t\text{Bu}_3\text{tach})\text{WS}_3]$, affording the product as a black solid (35 mg, 31%). Anal. Calcd. for $C_{33}H_{48}Fe_3N_3S_6SeW$: C, 35.72; H, 4.36; N, 3.79. Found: C, 35.51; H, 4.38; N, 3.77. ^{1}H NMR: δ 14.34 (*m*-H, 6), 3.31 (CH_2, 6), 2.48 (CH_3, 27), −3.64 (*o*-H, 6), −4.15 (*p*-H, 3).

In the sections following, clusters are numerically designated according to the Chart 1.

X-ray Structure Determinations. The structures of the 13 compounds in Tables 1 and 2 were determined. Diffraction-quality crystals were obtained by ether diffusion into acetonitrile solutions. Crystal mounting and data collections were performed as described[40] on a Bruker APEX II CCD single-crystal diffractometer. Data for compound **7b** were collected at the Advanced Photon Source. None of the crystals showed significant decay during the data collection procedure. Raw data were integrated and corrected for Lorentz and polarization effects using the Bruker APEX II program suite.[41] Absorption corrections were performed using SADABS. Space groups were assigned by analysis of symmetry and systematic absences (determined by XPREP) and were further checked by PLATON. Structures were solved by direct methods and refined against all data in the 2θ ranges by full-matrix least-squares on F^2 with the SHELXL program suite[42] using the OLEX 2 interface.[43] Hydrogen atoms at idealized positions were included in final refinements. The OLEX 2 interface was used for structure visualization and drawing ORTEP figures (shown in Figure 3 and 4). Refinement details and explanations (wherever necessary) are included in the

Table 2. Crystallographic Data for Compounds at 100 K[a]

	8b	9a	9b	10a	10b	11a
formula	$C_{18}H_{42}Fe_3MoN_3NaS_6Se \cdot 0.5(C_4H_{10}O)$	$C_{27}H_{57}Fe_3Mo\,N_6NaS_7 \cdot (C_4H_{10}O)$	$C_{27}H_{57}Fe_3Mo\,N_6NaS_6Se \cdot (C_4H_{10}O)$	$C_{33}H_{48}Fe_3Mo\,N_3S_7 \cdot 2(C_2H_3N)$	$C_{33}H_{48}Fe_3Mo\,N_3S_6Se \cdot 0.5(C_2H_3N)$	$C_{37}H_{54}Fe_3N_5S_7W$
formula weight	895.46	1050.88	1097.77	1056.83	1042.14	1144.67
crystal system	monoclinic	monoclinic	monoclinic	monoclinic	triclinic	monoclinic
space group	$P2_1/n$	$P2_1/n$	$P2_1/n$	$P2_1/n$	$P\bar{1}$	$P2_1/n$
Z	2	4	4	4	2	4
a, Å	9.9215(10)	13.1400(15)	13.1604(18)	13.137(3)	12.296(3)	13.1609(17)
b, Å	20.895(2)	18.913(2)	19.000(3)	20.952(5)	18.323(4)	20.997(3)
c, Å	17.3048(18)	19.779(2)	19.816(3)	16.063(4)	19.022(4)	16.036(2)
α, deg	90	90	90	90	81.471(3)	90
β, deg	91.424(2)	93.348(2)	93.553(2)	96.336(4)	76.904(3)	96.772(2)
γ, deg	90	90	90	90	78.096(3)	90
V, Å^3	3586.4(6)	4907.1(10)	4945.6(12)	4394.4(19)	4061.2(14)	4400.4(10)
d_{calcd}, g/cm^3	1.658	1.423	1.474	1.597	1.704	1.728
μ, mm^{-1}	2.925	1.456	2.138	1.616	2.587	3.941
max, min peaks, e Å^{-3}	2.818, −3.046	1.504, −1.406	1.585, −2.076	4.140, −1.396	3.149, −1.924	3.514, −1.718
2θ range, deg	3.06−51.38	3.62−51.36	3.76−51.4	3.20−51.46	3.00−51.62	3.68−51.38
R_1[b] (wR_2[c])	0.0683(0.1942)	0.0785(0.2070)	0.0778(0.1927)	0.0672(0.1573)	0.0732(0.1930)	0.0299(0.0803)
GOF ($F2$)	1.077	1.066	1.082	1.047	1.099	1.057

[a] Mo Kα radiation (λ = 0.71073 Å). [b] $R_1 = \Sigma||F_o| - |F_c||/\Sigma|F_o|$. [c] $wR_2 = \{\Sigma[w(F_o^2 - F_c^2)^2]/\Sigma[w(F_o^2)^2]\}^{1/2}$.

individual CIF files. Crystallographic data and final agreement factors are given in Tables 1 and 2.[44]

Other Physical Measurements. ^{1}H NMR spectra were obtained with a Varian M400 spectrometer in Me_2SO-d_6 solutions. Absorption spectra were measured on a Varian Cary 50 Bio spectrophotometer. ^{57}Fe Mössbauer spectra were measured with a constant acceleration spectrometer. Data were analyzed with Igor Pro 6 software (Wavemetrics, Portland, OR); isomer shifts are referenced to iron metal at room temperature. Cyclic voltammetry measurements were made with a BioAnalytical Systems Epsilon potentiostat/galvanostat in acetonitrile solutions at 100 mV/s using a glassy carbon working electrode, 0.1 M $(Bu_4N)(PF_6)$ supporting electrolyte, and an SCE reference electrode.

RESULTS AND DISCUSSION

Synthesis and Scope. In the cluster assembly systems of Figure 1, the trisulfido complexes $[(^tBu_3tach)M^{VI}S_3]$ (M = Mo, W) are utilized as scaffolds in which an intact MS_3 group is converted to the plausible heterometal unit $[MFe_3(\mu_3\text{-}S)_3]$ and the tridentate ^{t}Bu$_3$tach ligand blocks reaction at the M sites. This unit is capable of incorporating a fourth chalcogenide atom to complete the cubane-type core $[MFe_3S_3Q]^{3+,2+}$ (Q = S, Se). Preparation of **1a** and **1b** involves sulfide transfer to $[(^tBu_3tach)M^{VI}O_3]$ by Lawesson's reagent ($(p\text{-}MeOC_6H_4PS_2)_2$).[39] During reinvestigation of the isolation of **1a**, we obtained a molybdenum derivative of this reagent, $[(^tBu_3tach)MoO(\mu_2\text{-}S)_2(S)P(p\text{-}C_6H_4OMe)]$, whose X-ray structure suggests that it may be an intermediate in the reaction. Because no Mo or W complex with Lawesson's reagent has been obtained previously, we include the structure of this compound.[44]

The cluster assembly systems in Figure 1 consist of **1a** or **1b**, $FeCl_2$, Na_2Q, and NaSR in THF/acetonitrile. The quantity of thiolate controls the number of iron-bound ligands and core redox state as reflected by cluster charge, leading to isolation of the neutral clusters **3**, **4ab**, **6**, **10ab**, and **11ab** with 3+ cores and monanionic clusters **8ab** and **9ab** with 2+ cores. With **1b** only the neutral clusters **5ab**, **7ab**, and **11ab** have been isolated. Neutral clusters are formed under the generalized stoichiometry of reaction 1 (n = 1, 2, 4) and monoanionic clusters by reaction 2 (Q = S, Se for both) in which additional thiolate acts as a reductant. Under the conditions that afford reduced molybdenum clusters **9ab**, neutral tungsten clusters **7ab** are isolated. This result is apparently another manifestation of the greater difficulty in reducing the tungsten member of an isoligated isostructural Mo/W pair of complexes.[45]

$$\begin{aligned} &2\,[(^tBu_3tach)MS_3] + 6\,FeCl_2 + 2n\,NaSPh \\ &\quad + 2\,Na_2Q \rightarrow 2\,[(^tBu_3tach)MFe_3S_3QCl_{4-n}(SPh)_{n-1}] \\ &\quad + PhSSPh + 2(n+2)\,NaCl \end{aligned} \tag{1}$$

$$\begin{aligned} &[(^tBu_3tach)MS_3] + 3\,FeCl_2 + 5\,NaSR \\ &\quad + Na_2Q \rightarrow Na[(^tBu_3tach)MFe_3S_3Q(SR)_3] \\ &\quad + RSSR + 6\,NaCl \end{aligned} \tag{2}$$

The cubane clusters exhibit isotropically shifted ^{1}H NMR spectra as a consequence of paramagnetism, presumably similar to that of the $[MoFe_3S_4]^{3+}$ ($S = 3/2$[46]) and $[MoFe_3S_4]^{2+}$ (S = 2[46,47]) oxidation states determined for other clusters. These spectra, four of which (**7b**, **8a**, **9a**, **11a**) encompassing both oxidation states, are included in Figure 2, are useful in cluster identification. The alternating signs of the o-H (+10.9 ppm), m-H (−7.0 ppm), and p-H (+11.1 ppm) isotropic shifts of benzenethiolate cluster **11a** indicate that these shifts are dominantly contact in origin.[48] The same behavior is exhibited by **4ab**, **5ab**, **10ab**, and **11b.** The spectrum of methanethiolate cluster **8a** (−9.67 ppm) leads the assignment of the CH_2 (−9.32 ppm)) and CH_3 (9.60 ppm) signals of ethanethiolate cluster **9a** and also **6**, **7ab**, and **9b.** While these spectra could have been assigned on

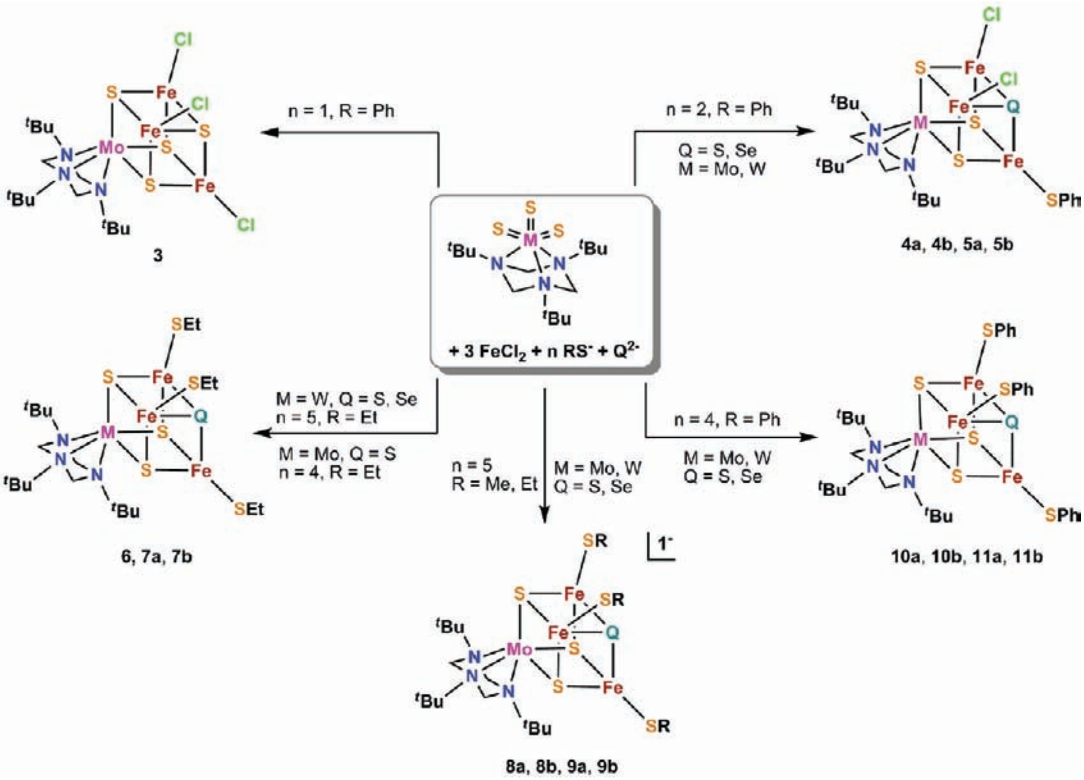

Figure 1. Schematic depiction of the synthesis of (Mo/W)-Fe-(S/Se) clusters.

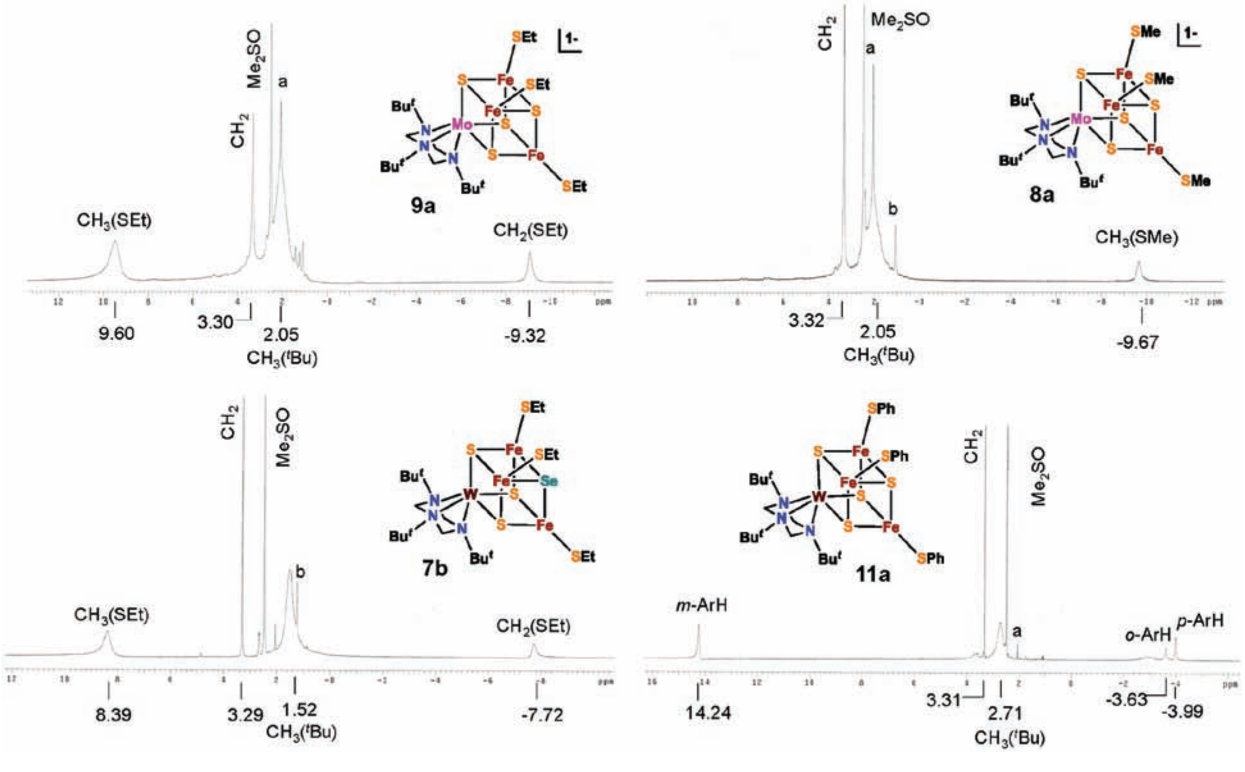

Figure 2. ^{1}H NMR spectra of representative clusters in Me$_2$SO-d$_6$. Signal assignments are indicated. Peaks denoted as a and b are CH_3CN and $(CH_3CH_2)_2$O respectively.

the basis of relative intensities, the oppositely signed isotropic shifts of the SEt group (CH$_2$, −8.57 ppm; CH$_3$, +11.52 ppm) are unexpected. Nearly always, contact shifted proton resonances of *n*-alkyl groups attenuate along the chain with the same sign in the

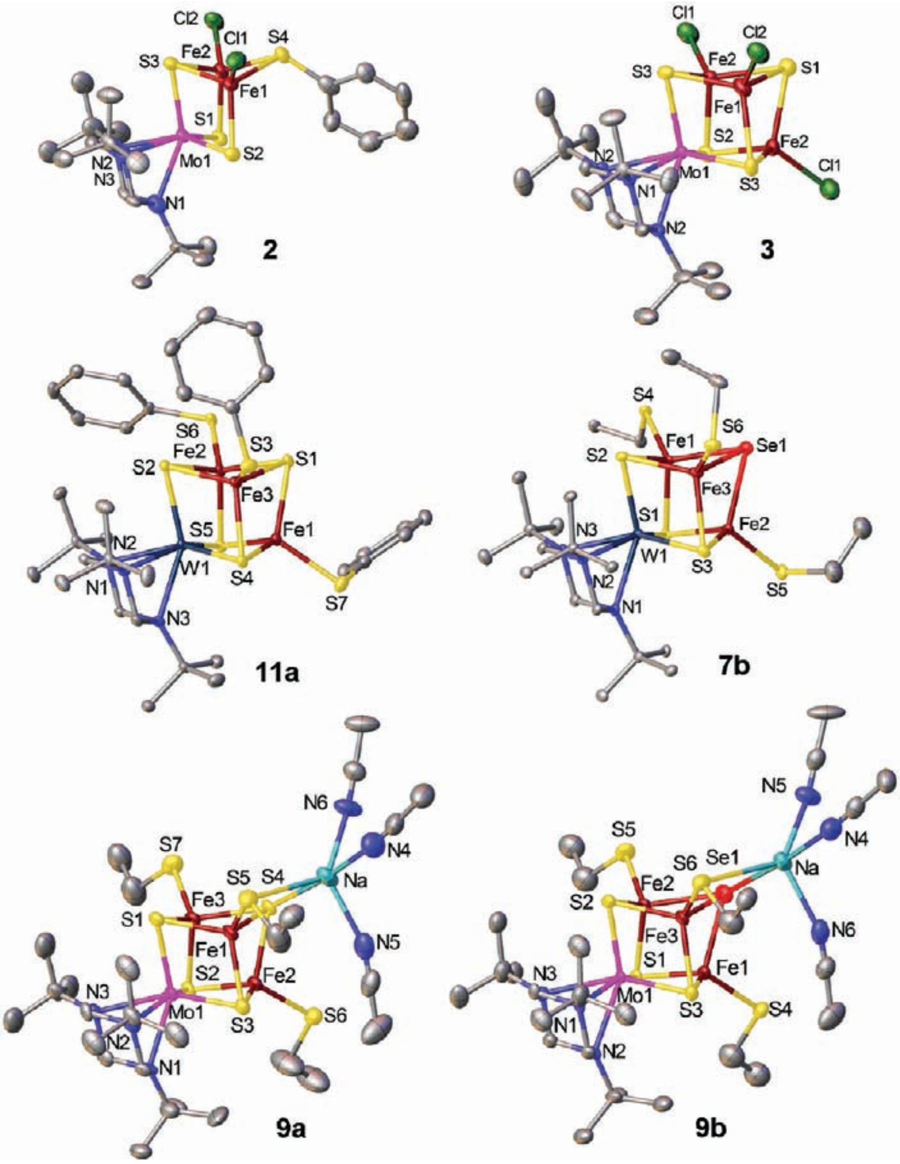

Figure 3. Structures of single cubanes (**2**, **3**, **7b**, **9a**, **9b**, and **11a**) shown with 50% probability ellipsoids and partial atom labeling schemes. Hydrogen atoms are omitted for clarity.

absence of dipolar contributions to the shifts, a behavior observed for other $[MoFe_3S_4]^{3+}$ clusters.[49−51] The first examples of ^{1}H NMR spectra of $[MoFe_3S_4]^{2+}$ clusters with alkylthiolate ligands are reported here.

Also prepared in this work, by means of reaction 3, is the incomplete cubane **2**, so designated because of the vacancy of an iron atom in one vertex of a cubane.

$$\begin{aligned} &2\,[(^t\mathrm{Bu_3tach})\mathrm{MoS_3}] + 4\,\mathrm{FeCl_2} \\ &\quad + 4\,\mathrm{NaSPh} \rightarrow 2\,[(^t\mathrm{Bu_3tach})\mathrm{MoFe_2S_3Cl_2(SPh)}] \\ &\quad + \mathrm{PhSSPh} + 4\,\mathrm{NaCl} \end{aligned} \tag{3}$$

The cluster, shown in Figure 3, may be considered as a trapped intermediate in the cluster assembly process. Once the μ_2-SPh bridge is formed, cubane formation does not proceed, and **2** is isolated as a stable Et_4N^+ salt. On occasion, cubane **3** is found as an impurity in the preparation of **2** and conversely. The X-ray structure of one crystal contained both **2** and **3**.[44] Cluster **3** has also been isolated in low yield by reaction 1 with no externally added Na_2S, indicating that initial complex **1a** is susceptible to sulfide extraction. This event may lead to undesirable side reactions and may contribute to the observed moderate yields (ca. 30−50%) of the cubane clusters. However, all compounds were isolated by essentially the same procedure as crystalline solids that meet analytical and/or ^{1}H NMR standards of purity, and are readily accessible.

Cluster Structures. The cubane formulation of clusters has been verified by X-ray structure determinations of 12 compounds. Structures (except **6**) are presented in Figures 3 and 4. Bond distances and angles involving variable atom Q = S, Se are collected in Table 3 together with cluster volumes calculated from atom coordinates. Other bond distances and angles are unexceptional and are available elsewhere.[44] We make several brief observations. (i) Mo−S and W−S distances in the entire set of clusters occur in the range 2.29−2.35 Å, and are substantially longer than the Mo^{VI}−S distance of 2.173(6) Å in **1a**,[39] a

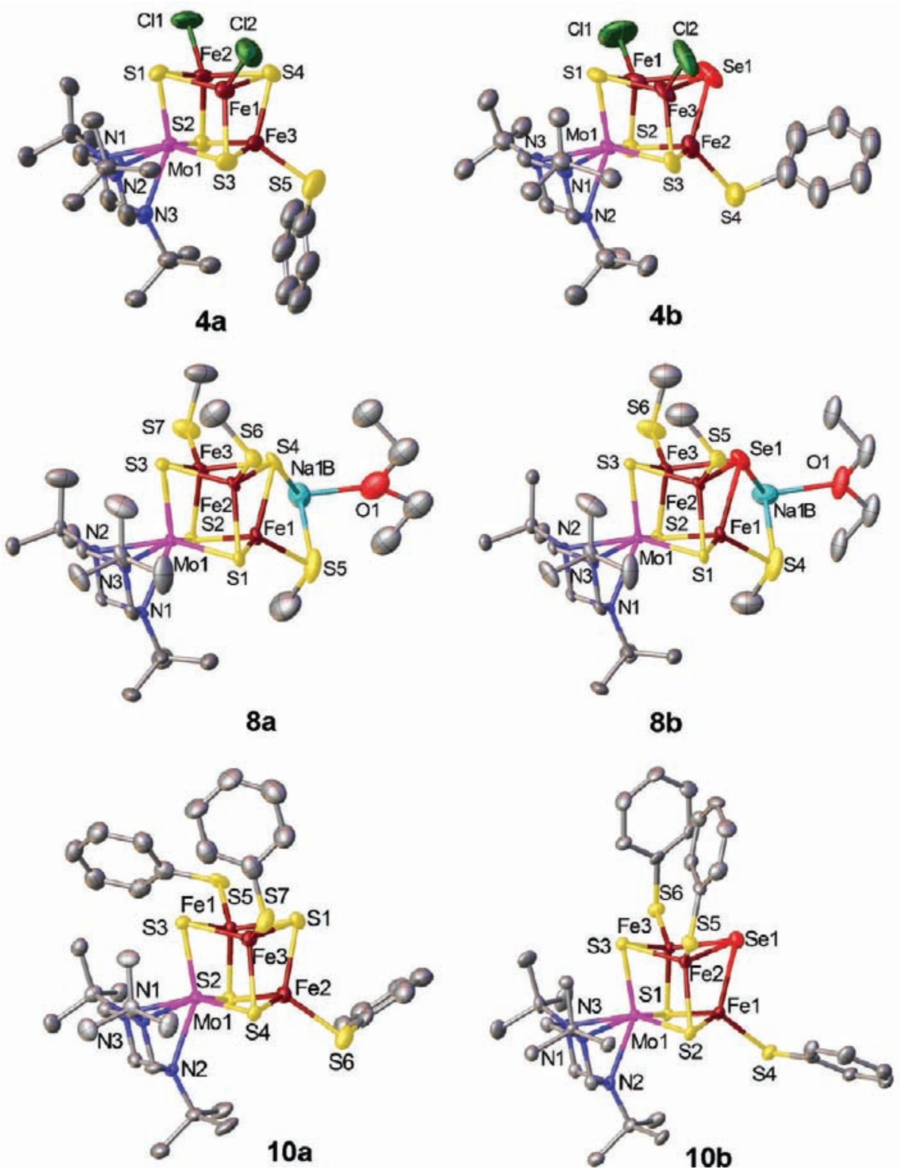

Figure 4. Structures of single cubanes (**4a**, **4b**, **8a**, **8b**, **10a**, and **10b**) shown with 50% probability ellipsoids and partial atom labeling schemes. Hydrogen atoms are omitted for clarity. **8a** and **8b** exist in dimeric forms involving two sodium atoms each coordinated with diethylether molecule of one-half occupancy.

behavior consistent with reduction to the $M^{III/IV}$ level in reactions 1−3. (ii) N−M−N angles are nearly invariant at 59.5−61.3° and correspond closely to those in other $M^{0,IV,VI}$ complexes (58−61°) with the same ligand.[39,52,53] These angles, dictated by the 6-membered ring of ^{t}Bu$_3$tach, suggest chelate ring strain larger than that in the less trigonally distorted, generally robust complexes of the type $[M^{III-VI}(Me_3tacn)L_3]^z$ in which the ligand is a 9-membered ring with N−M−N angles in the range 73−79° (M = Mo, W).[39,54−57] Ring detachment owing to strain may occur during synthesis, but the binding is sufficient to allow serviceable yields. (iv) Structurally comparable pairs of clusters **4ab**, **8ab**, **9ab**, and **10ab** differ only in atom Q and afford the bond length and angle orders Fe−Se > Fe−S and Fe−S−Fe > Fe−Se−Fe for individual and mean values. Although the standard deviation of mean bond lengths is large, the differences between comparable pairs is 0.10−0.13 Å; likewise, the difference between angles is 1.6−3.4°.

Oxidation States and Charge Distribution. A property of interest in heterometal iron-sulfur clusters is charge distribution as approximated by metal oxidation states. The procedure in this laboratory is to determine iron (mean) oxidation states by ^{57}Fe isomer shifts and infer that of the heterometal by difference. Mössbauer spectra of eight clusters were measured at 100 K; isomer shifts (δ) and quadrupole splittings are listed in Table 4. All spectra consist of a single quadrupole doublet, indicating delocalized electronic structures of these mixed valence clusters. Iron oxidation states s were calculated from the empirical relation $\delta = 1.43 - 0.40s$ which applies to tetrahedral FeS_4 sites at or near 77 K.[4] The values s = 2.33+ and 2.67+ correspond to the formal designations $M^{3+}Fe^{2+}{}_2Fe^{3+}$ and $M^{3+}Fe^{2+}Fe^{3+}{}_2$, respectively. Reduced clusters **9a** (2.32+) and **9b** (2.40+) belong to the first designation. Oxidized clusters **8a** and **10a** (both 2.67+), as practically all $[MFe_3S_4]^{3+}$ clusters examined in this laboratory, belong to the second one. The empirical relationship does not

Table 3. Selected Bond Distances, Angles, and Core Volumes

	Fe–Q bond distances[b] (Å)		Fe–Q–Fe angles[b] (deg)	
compounds[a]	Q = S	Q = Se	Q = S	Q = Se
3	2.267(3), 2.299(3)[c], 2.299(3)[c]		72.75(9)[c], 72.75(9)[c], 71.3(1)	
4a	2.234(3), 2.255(3), 2.264(4)		71.4(1), 71.4(1), 71.62(10)	
4b		2.339(2), 2.382(2), 2.418(3)		68.25(7), 70.60(7), 70.77(7)
6	2.249(7), 2.235(6), 2.322(7)		73.8(2), 71.7(2), 71.0(2)	
7b		2.349(3), 2.413(3), 2.424(3)		67.43(8), 69.81 (8), 70.46(8)
8a	2.264(2), 2.303(2), 2.331(2)		69.12(5), 71.70(5), 73.11(6)	
8b		2.388(2), 2.389(2), 2.412(2)		66.90(4), 68.88(5), 70.12(5)
9a	2.270(3), 2.328(2), 2.336(3)		69.98(8), 71.99(8), 72.55(8)	
9b		2.367(2), 2.425(2), 2.434(2)		67.05(5), 69.40(5), 69.90(5)
10a	2.236(2), 2.287(3), 2.315(3)		70.99(8), 73.21(8), 73.75(8)	
10b		2.326(2), 2.400(2), 2.410 (2)		67.64(5), 70.03(5), 70.06 (5)
11a	2.220(1), 2.292(1), 2.306(1)		70.97(3), 73.24(3), 74.11(3)	

	core volumes (Å^3)		
	MFe_3	Q_4	MFe_3Q_4
9a	2.34	5.72	9.46
9b	2.36	5.94	9.64
10a	2.33	5.57	9.35
10b	2.33	5.83	9.49

[a] M = Mo except **7b** and **11a** (M = W). [b] See Figure 1 for position of Q in clusters. [c] Equal by symmetry element.

Table 4. Mössbauer Parameters (100 K) for Selected Clusters

compounds	δ (mm/s)[a]	ΔE_Q (mm/s)
4a	0.42	0.88
4b	0.45	0.84
7b	0.44	0.88
8a	0.36	0.76
9a	0.50	1.12
9b	0.47	0.99
10a	0.36	0.76
10b	0.41	0.83

[a] Referenced with Fe metal at room temperature.

strictly apply to **4ab** because of chloride ligation. Values for **7b** and **10b** are intermediate, and no conclusions can be drawn.

Sulfur vs Selenium. The difference in ionic radii between Se^{2-} and S^{2-} is 1.91 − 1.84 = 0.07 Å and between covalent radii is 1.17 − 1.04 = 0.13 Å.[58] These differences are reflected in the preceding bond distance and angle orders, which are characteristic of all comparative pairs of S/Se compounds of any type in which only atom Q is varied. A further indication of these effects is seen in the core volumes of two comparative pairs, **9ab** and **10ab**. While values of the MFe_3 tetrahedra are practically invariant, the entire core MFe_3Q_4 volume increases by 1.9% (**9ab**) and 1.5% (**10ab**). The effect is small and expectedly smaller than replacing 4S with 4Se, as in the pair $[Fe_4Q_4(SPh)_4]^{2-}$ where the core volumes are 9.55 Å^3 (Q = S)[59] and 10.54 Å^3 (Q = Se),[25] a 10.4% increase. Other properties are summarized in Figure 5 for the comparative pair **9ab** as an example. The energy of the charge transfer band near 380 nm is unchanged, and band intensites are only slightly affected. The clusters show two chemically reversible redox steps in the −0.7 to −2.0 V range with the potentials of the selenium-containing cluster being more positive[25] by 10 and 50 mV. Mössbauer spectra are nearly the same, and isomer shifts are within experimental uncertainty of about ± 0.02 mm/s.

Summary. This report describes the synthesis, characterization, and comparative study of isostructural Mo/W−Fe−S single cubane clusters that differ by only one vertex atom Q = S or Se. The following are the principal results and findings of this investigation.

(1) A new self-assembly system has been developed for heterometal-iron-sulfur single cubane clusters that allows selective incorporation of sulfide or selenide at one vertex of the structure. The method utilizes as templates the compounds $[(^tBu_3tach)M^{VI}S_3]$ (M = Mo, W), which furnish three of the four chalcogenide atoms in the product cubane core $[MFe_3S_3Q]$ as the MS_3 fragment.

(2) An extensive series of clusters with the cores $[MFe_3S_3Q]^{3+,2+}$ has been prepared by assembly reactions 1 and 2 (30−50% purified yields) and characterized by X-ray structure determinations. The presence of Q = Se retains the cubane structure with small changes in bond distances and angles that are intrinsic to the structural behavior of selenium vs sulfur.

(3) A possible trapped intermediate $[(^tBu_3tach)MoFe_2S_3Cl_2(\mu_2\text{-}SPh)]$ in the assembly process has been isolated and shown to have an incomplete cubane structure with one vertex iron atom missing.

(4) On the basis of the comparative properties of $[(^tBu_3tach)MoFe_3S_3Q(SEt)_3]^{1-}$, the Q = Se atom produces an about 2% increase in core volume, slightly less negative redox potentials (less easily oxidized), and virtually no change in ^{57}Fe isomer shift or UV−visible absorption spectrum. Isomer shifts indicate that both clusters correspond to the $M^{3+}Fe^{2+}{}_2Fe^{3+}$ oxidation state formalism.

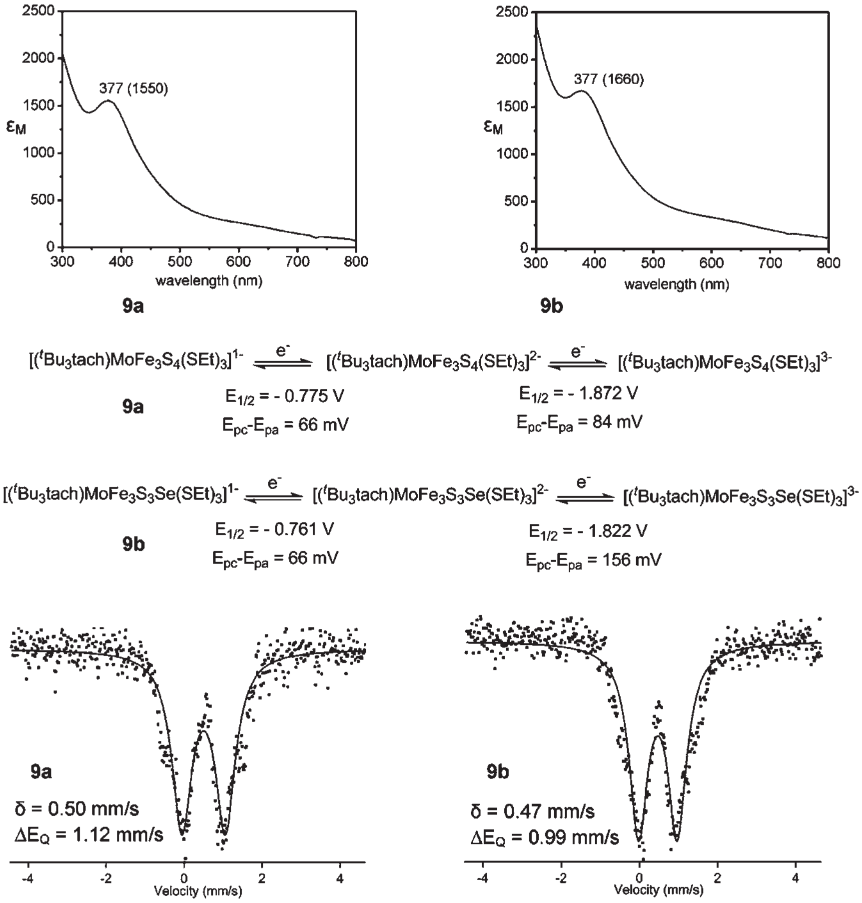

Figure 5. Absorption spectra (in acetonitrile), redox couples (in acetonitrile), and Mössbauer spectra (100 K) of complexes **9a** and **9b**.

These findings are consistent with the properties of the pair $[Fe_4Q_4(SPh)_4]^{2-}$ for which, however, the effects of selenide become more pronounced because of complete chalcogenide substitution.[25]

The existence of the cluster $[Fe_4S_3(N^tBu)Cl_4]^{2-}$ [38] makes evident the ability of weak-field cubane sterechemistry to incorporate a much smaller nonsulfur atom (Fe—N 1.95 Å) in addition to sulfide itself (mean Fe—S 2.31(4) in **9a**) and the larger selenide (mean Fe—Se 2.41(4) in **9b**). This raises the possibility that anions containing oxygen or nitrogen may be incorporated as μ_3 bridges using the methods employed in this work. This investigation is underway. Thereafter, it remains to be learned if nonsulfur bridge atoms can be introduced in larger structures and manipulated into an interstitial position by core rearrangement.

■ ASSOCIATED CONTENT

Ⓢ Supporting Information. X-ray crystallographic files in CIF form for all compounds in Tables 1 and 2, depiction of additional cluster structures, and additional ^1H NMR and Mössbauer spectra. This material is available free of charge via the Internet at http://pubs.acs.org.

■ AUTHOR INFORMATION

Corresponding Author

*E-mail: holm@chemistry.harvard.edu.

■ ACKNOWLEDGMENT

This research was supported by NIH Grant GM-28856. We thank Dr. Shao-Liang Zheng for his help with X-ray data collection and structure determinations. We thank Prof. S. C. Lee for volume calculations and Dr. Yu-Sheng Chen at ChemMat CARS, Advanced Photon Source, Argonne National Laboratory, for his assistance with single crystal data for compound **7b**. ChemMat CARS Sector 15 is principally supported by the National Science Foundation/Department of Energy under Grant NSF/CHE-0822838. Use of the Advanced Photon Source was supported by the Department of Energy, Office of Science, Office Basic Energy Sciences, under Contract No. DE-AC02-06CH11357.

■ REFERENCES

(1) Lee, S. C.; Holm, R. H. *Chem. Rev.* **2004**, *104*, 1135–1157.
(2) Pryadun, R.; Holm, R. H. *Inorg. Chem.* **2008**, *47*, 3366–3370.
(3) Holm, R. H. Iron-Sulfur Clusters. In *Bio-coordination Chemistry*; Que, L., Jr., Tolman, W. A., Eds.; Elsevier: Oxford, 2004; pp 61–90.
(4) Rao, P. V.; Holm, R. H. *Chem. Rev.* **2004**, *104*, 527–559.
(5) Sharp, C. R.; Duncan, J. S.; Lee, S. C. *Inorg. Chem.* **2010**, *49*, 6697–6705.
(6) Holm, R. H.; Simhon, E. D. In *Molybdenum Enzymes*; Spiro, T. G., Ed.; Wiley: New York, 1985; pp 1–87.
(7) Fomitchev, D. V.; McLauchlan, C. C.; Holm, R. H. *Inorg. Chem.* **2002**, *41*, 958–966.
(8) Kovacs, J. A.; Holm, R. H. *Inorg. Chem.* **1987**, *26*, 702–711.
(9) Ciurli, S.; Ross, P. K.; Scott, M. J.; Yu, S.-B.; Holm, R. H. *J. Am. Chem. Soc.* **1992**, *114*, 5415–5423.

(10) Panda, R.; Berlinguette, C. P.; Zhang, Y.; Holm, R. H. *J. Am. Chem. Soc.* **2005**, *127*, 11092–11101.

(11) Zhou, H.-C.; Holm, R. H. *Inorg. Chem.* **2003**, *42*, 11–21.

(12) Deng, L.; Holm, R. H. *J. Am. Chem. Soc.* **2008**, *130*, 9878–9886.

(13) Demadis, K. D.; Campana, C. F.; Coucouvanis, D. *J. Am. Chem. Soc.* **1995**, *117*, 7832–7833.

(14) Berlinguette, C. P.; Miyaji, T.; Zhang, Y.; Holm, R. H. *Inorg. Chem.* **2006**, *45*, 1997–2007.

(15) Scott, T. A.; Holm, R. H. *Inorg. Chem.* **2008**, *47*, 3426–3432.

(16) Zhang, Y.; Holm, R. H. *J. Am. Chem. Soc.* **2003**, *125*, 3910–3920.

(17) Berlinguette, C. P.; Holm, R. H. *J. Am. Chem. Soc.* **2006**, *128*, 11993–12000.

(18) Zuo, J.-L.; Zhou, H.-C.; Holm, R. H. *Inorg. Chem.* **2003**, 4624–4631.

(19) Ohki, Y.; Ikagawa, Y.; Tatsumi, K. *J. Am. Chem. Soc.* **2007**, *129*, 10457–10465.

(20) Ohki, Y.; Imada, M.; Murata, A.; Sunada, Y.; Ohta, S.; Honda, M.; Sasamori, T.; Katada, M.; Tatsumi, K. *J. Am. Chem. Soc.* **2009**, *131*, 13168–13178.

(21) Hashimoto, T.; Ohki, Y.; Tatsumi, K. *Inorg. Chem.* **2010**, *49*, 6102–6109.

(22) Peters, J. W.; Stowell, M. H. B.; Soltis, S. M.; Finnegan, M. G.; Johnson, M. K.; Rees, D. C. *Biochemistry* **1997**, *36*, 1181–1187.

(23) Mayer, S. M.; Lawson, D. M.; Gormal, C. A.; Roe, S. M.; Smith, B. E. *J. Mol. Biol.* **1999**, *292*, 871–891.

(24) Einsle, O.; Tezcan, F. A.; Andrade, S. L. A.; Schmid, B.; Yoshida, M.; Howard, J. B.; Rees, D. C. *Science* **2002**, *297*, 1696–1700.

(25) Bobrik, M. A.; Laskowski, E. J.; Johnson, R. W.; Gillum, W. O.; Berg, J. M.; Hodgson, K. O.; Holm, R. H. *Inorg. Chem.* **1978**, *17*, 1402–1410.

(26) Reynolds, J. G.; Holm, R. H. *Inorg. Chem.* **1981**, *20*, 1873–1878.

(27) Rutchik, S.; Kim, S.; Walters, M. A. *Inorg. Chem.* **1988**, *27*, 1513–1515.

(28) Carney, M. J.; Papaefthymiou, G. C.; Whitener, M. A.; Spartalian, K.; Frankel, R. B.; Holm, R. H. *Inorg. Chem.* **1988**, *27*, 346–352.

(29) Stack, T. D. P.; Weigel, J. A.; Holm, R. H. *Inorg. Chem.* **1990**, *29*, 3745–3760.

(30) Yu., S.-B.; Papaefthymiou, G. C.; Holm, R. H. *Inorg. Chem.* **1991**, *30*, 3476–3485.

(31) Zhou, C.; Holm, R. H. *Inorg. Chem.* **1997**, *36*, 4066–4077.

(32) Kornienko, A.; Huebner, L.; Freedman, D.; Emge, T. J.; Brennan, J. G. *Inorg. Chem.* **2003**, *43*, 8476–8480.

(33) Kern, A.; Näther, C.; Studt, F.; Tuczek, F. *Inorg. Chem.* **2004**, *43*, 5003–5010.

(34) Hauptmann, R.; Schneider, J.; Chen, C.-N.; Henkel, G. *Acta Crystallogr.* **1999**, *C55*, 192–194.

(35) Greaney, M. A.; Coyle, C. L.; Pilato, R. S.; Stiefel, E. I. *Inorg. Chim. Acta* **1991**, *189*, 81–96.

(36) Verma, A. K.; Lee, S. C. *J. Am. Chem. Soc.* **1999**, *121*, 10838–10839.

(37) Zdilla, M. J.; Verma, A. K.; Lee, S. C. *Inorg. Chem.* **2011**, *50*, 1551–1562.

(38) Chen, X.-D.; Duncan, J. S.; Verma, A. K.; Lee, S. C. *J. Am. Chem. Soc.* **2010**, *132*, 15884–15886.

(39) Partyka, D. V.; Staples, R. J.; Holm, R. H. *Inorg. Chem.* **2003**, *42*, 7877–7886.

(40) Groysman, S.; Holm, R. H. *Inorg. Chem.* **2007**, *46*, 4090–4102.

(41) *APEX II*, v. 2009; Bruker Analytical X-ray Systems, Inc.: Madison, WI, 2009.

(42) Sheldrick, G. M. *Acta Crystallogr.* **2009**, *A64*, 112–122.

(43) Dolomanov, O. V.; Bourhis, L. J.; Gildea, R. J.; Howard, J. A. K.; Puschmann, H. *J. Appl. Crystallogr.* **2009**, *42*, 339–341.

(44) See paragraph at the end of the article concerning Supporting Information available.

(45) Holm, R. H.; Solomon, E. I.; Majumdar, A.; Tenderholt, A. *Coord. Chem. Rev.* **2011**, *255*, 993–1015.

(46) Mascharak, P. K.; Papaefthymiou, G. C.; Armstrong, W. H.; Foner, S.; Frankel, R. B.; Holm, R. H. *Inorg. Chem.* **1983**, *22*, 2851–2858.

(47) Xi, B.; Holm, R. H. *Inorg. Chem.* **2011**, *50*, 6280–6288.

(48) Holm, R. H.; Phillips, W. D.; Averill, B. A.; Mayerle, J. J.; Herskovitz, T. *J. Am. Chem. Soc.* **1974**, *96*, 2109–2117.

(49) Wolff, T. E.; Berg, J. M.; Holm, R. H. *Inorg. Chem.* **1981**, *20*, 174–180.

(50) Armstrong, W. H.; Mascharak, P. K.; Holm, R. H. *J. Am. Chem. Soc.* **1982**, *104*, 4373–4383.

(51) Zhang, Y.-P.; Bashkin, J. K.; Holm, R. H. *Inorg. Chem.* **1987**, *36*, 694–702.

(52) Armanasco, N. L.; Baker, M. V.; North, M. R.; Skelton, B. W.; White, A. H. *J. Chem. Soc., Dalton Trans.* **1998**, 1145–1149.

(53) Baker, M. V.; North, M. R.; Skelton, B. W.; White, A. H. *Inorg. Chem.* **1999**, *38*, 4515–4521.

(54) Backes-Dahmann, G.; Herrmann, W.; Wieghardt, K.; Weiss, J. *Inorg. Chem.* **1985**, *24*, 485–491.

(55) Bürger, K. S.; Haselhorst, G.; Stötzel, S.; Weyhermüller, T.; Wieghardt, K.; Nuber, B. *J. Chem. Soc., Dalton Trans.* **1993**, 1987–1997.

(56) Shores, M. P.; Sokol, J. J.; Long, J. R. *J. Am. Chem. Soc.* **2002**, *124*, 2279–2292.

(57) Wieghardt, K.; Backes-Dahmann, G.; Nuber, B.; Weiss, J. *Angew. Chem., Int. Ed. Engl.* **1985**, *24*, 777–778.

(58) Emsley, J. *The Elements*, 3rd ed.; Oxford University Press: Oxford, 1998; pp 188, 198.

(59) Que, L., Jr.; Bobrik, M. A.; Ibers, J. A.; Holm, R. H. *J. Am. Chem. Soc.* **1974**, *96*, 4168–4178.